Protein Science (1996), 5:2287–2297. Cambridge University Press. Printed in the USA.

Secondary structure, membrane localization, and coassembly within phospholipid membranes of synthetic segments derived from the N- and C-termini regions of the ROMK1 K^+ channel

IRIS BEN-EFRAIM AND YECHIEL SHAI

Department of Membrane Research and Biophysics, Weizmann Institute of Science, Rehovot, 76100 Israel

(RECEIVED May 21, 1996; ACCEPTED August 19, 1996)

Abstract

The hydropathy plot of the inwardly rectifying ROMK1 K^+ channel, which reveals two transmembrane and a pore region domains, also reveals areas of intermediate hydrophobicity in the N terminus (M0) and in the C terminus (post-M2). Peptides that correspond to M0, post-M2, and a control peptide, pre-M0, were synthesized and characterized for their structure, affinity to phospholipid membranes, organizational state in membranes, and ability to self-assemble and coassemble in the membrane-bound state. CD spectroscopy revealed that both M0 and post-M2 adopt highly α-helical structures in 1% SDS and 40% TFE/water, whereas pre-M0 is not α-helical in either 1% SDS or 40% TFE/water. Binding experiments with NBD-labeled peptides demonstrated that both M0 and post-M2, but not pre-M0, bind to zwitterionic phospholipid membranes with partition coefficients of 10^3–10^5 M^{-1}. A surface localization for both post-M2 and M0 was indicated by NBD shift, tryptophan quenching experiments with brominated phospholipids, and enzymatic cleavage. Resonance energy transfer measurements between fluorescently labeled pairs of donor (NBD)/acceptor (rhodamine) peptides revealed that M0 and post-M2 can coassemble in their membrane-bound state, but cannot self-associate when membrane-bound. The results are in agreement with recent data indicating that amino acids in the carboxy terminus of inwardly rectifying K^+ channels have a major role in specifying the pore properties of the channels (Taglialatela M, Wible BA, Caporaso R, Brown AM, 1994, *Science 264*:844–847; Pessia M, Bond CT, Kavanaugh MP, Adelman JP, 1995, *Neuron 14*:1039–1045). The relevance of the results presented herein to the suggested model for the structure of the ROMK1 channel and to general aspects of molecular recognition between membrane-bound polypeptides are also discussed.

Keywords: channel structure; fluorescence; K^+ channels; synthetic peptides

Inwardly rectifying K^+ channels conduct an inward K^+ current at hyperpolarizing membrane potentials. These channels, because of their rectification properties, play an important role in regulating the resting membrane potential and electrical excitability of cells in a variety of tissues, including the brain and heart (Hille, 1992). The recent cDNA cloning in *Xenopus* oocytes of several inwardly rectifying K^+ channels, namely ROMK1 (Ho et al., 1993; Shuck et al., 1994), IRK1 (Kubo et al., 1993a; Koyama et al., 1994), GIRK1/KGB (Dascal et al., 1993; Kubo et al., 1993b), HRK/HIR (Makhina et al., 1994; Perier et al., 1994), K_{ATP} (Ashford et al., 1994), and BIRK (Bredt et al., 1995), has enabled a look at the primary structure of these channels. Hydropathy plots have suggested only two potential transmembrane domains, M1 and M2, and a pore-forming region, H5, which is involved in ion conductance (Fig. 9A) (Ho et al., 1993). For voltage-dependent K^+ channels, six transmembrane segments (S1–S6) have been postulated (Papazian et al., 1987). The H5 domain is highly homologous between inwardly rectifying K^+ channels and voltage gated K^+ channels. A small degree of similarity between M1 and S5 and between M2 and S6 also exists. Based on this homology, it was

Reprint requests to: Yechiel Shai, Department of Membrane Research and Biophysics, Weizmann Institute of Science, Rehovot, 76100 Israel; e-mail: bmshai@weizmann.weizmann.ac.il.

Abbreviations: BOC, butyloxycarbonyl; 6,7-BrPC, 1-palmitoyl-2-stearoyl(6-7) dibromo-sn-glycero-3 phosphocholine; 9,10-BrPC, 1-palmitoyl-2-stearoyl(9-10) dibromo-sn-glycero-3 phosphocholine; 11,12-BrPC, 1-palmitoyl-2-stearoyl(11-12) dibromo-sn-glycero-3 phosphocholine; DCC, dicyclohexylcarbodiimide; DIEA, diisopropylethylamine; DMF, dimethyl formamide; HF, hydrogen fluoride; HOBT, 1-hydroxybenzotriazole; LUV, large unilamellar vesicles; NBD, 7-nitrobenz-2-oxa-1,3-diazole, 4-yl; Pam, (phenylacetamido)methyl; NBD-F, 4-fluoro-7-nitrobenz-2-oxa-1,3-diazole; PC, egg phosphatidylcholine; Rho, tetramethylrhodamine; Rho-Su, 5-(and-6)-carboxytetramethylrhodamine succinimidyl ester; RP-HPLC, reverse-phase HPLC; SUV, small unilamellar vesicles; TFA, trifluoroacetic acid; TFE, trifluoroethanol.

suggested that inwardly rectifying channels are structurally analogous to the inner core of the *Shaker* superfamily of K^+ channels (Kubo et al., 1993a; Bredt et al., 1995). However, hydropathy plots of the inwardly rectifying K^+ channels reveal areas of intermediate hydrophobicity in the extended C-terminal region (Taglialatela et al., 1994) and the shorter N-terminal region (Ho et al., 1993), which are reminiscent of the degree of hydrophobicity of H5, a region that was believed initially to be extracellular (Catterall, 1988). Based on experimental results, it has been suggested that, in inwardly rectifying channels, parts of the C terminus are likely to be in the membrane and that the C terminus makes a major contribution to the pore (Taglialatela et al., 1994; Pessia et al., 1995).

A connection between inwardly rectifying K^+ channels and voltage-gated K^+ channels possibly exists. Deletion of transmembrane domains S1–S4 converts a depolarization-activated wild-type Kv1.1 K^+ channel with outward rectification into a hyperpolarization-activated channel exhibiting inward rectification. Although the pore region of the deletion mutant is identical to that of the wild-type channel, the mutant channel is a nonselective cation channel and is characterized by an altered pharmacologic profile (Tytgat et al., 1994; Van de Voorde & Tytgat, 1995). This phenotypical change, which is associated with the removal of the transmembrane domains S1–S4, further suggests a structural similarity between inwardly rectifying K^+ channels and the *Shaker* superfamily of ion channels. Interestingly, unlike mammalian inwardly rectifying K^+ channels, plant inwardly rectifying K^+ channels consist of six putative transmembrane domains, similar to animal voltage gated channels of the *Shaker* superfamily (Very et al., 1994).

Whether parts of the ROMK1 channel adjacent to the pore region are indeed involved in the formation of the hydrophobic core of this channel was tested by synthesizing segments from its N and C termini, labeling them with fluorescent probes, and investigating their structures in hydrophobic environments, their affinity to phospholipid membranes, and their organization when in the membrane-bound state. We present evidence that the M0 and post-M2 segments bind strongly to phospholipid membranes, and that they adopt highly α-helical structures in membrane mimetic environments, whereas pre-M0 neither binds to the membrane nor adopts an α-helical structure. Furthermore, M0 and post-M2 cannot self-associate, but can coassemble in their membrane-bound state. The results are discussed with respect to the suggested model for the organization of the ROMK1 channel and to general aspects of molecular recognition between membrane-bound polypeptides.

Results

Peptides that correspond to regions of the C- and N-termini domains of ROMK1 channel were synthesized, labeled fluorescently, and their structure, affinity to phospholipid membranes, and organization in the membrane-bound state studied. M0, which corresponds to residues 58–80 of the N terminus, is composed of 23 amino acids. Post-M2, which corresponds to residues 198–223 of the C terminus, is composed of 26 amino acids. Another peptide, pre-M0, was synthesized to serve as a control and is composed of the 22 amino acids (residues 36–57) preceding M0. These three sequences were chosen according to the Kyte and Doolittle hydropathy plot of ROMK1 (Kyte & Doolittle, 1982; Ho et al., 1993) and contained short extensions of the termini. Previous studies have shown that extension or truncation by several amino acids at either end of a membrane polypeptide does not significantly alter its structure and ability to bind to phospholipid membranes (Ben-Efraim et al., 1993, 1994). Fluorescently labeled analogues of the three peptides were prepared by modifying their N-terminal amino acids selectively with a fluorescent probe, either NBD (to serve in the binding experiments and as an energy donor) or Rho (an energy acceptor). Post-M2 was also labeled with NBD at its C-terminal amino acid. NBD and rhodamine labeling of biologically active polypeptides (Pouny et al., 1992; Rapaport & Shai, 1992) and transmembrane segments of membrane proteins (Gazit & Shai, 1993a, 1995) does not affect their function significantly. The sequences of the peptides, their fluorescently labeled analogues, and their designations are given in Table 1, and their location within the sequence of the channel is shown in Figure 9A.

CD spectroscopy

The extent of the α-helical secondary structure of the peptides was estimated from their CD spectra, as measured in 40% TFE (Fig. 1A) and in 1% SDS (Fig. 1B). M0 and post-M2 exhibited significant CD signals, whereas pre-M0 did not. The mean residual ellipticities at $[\Theta]_{222}$ for M0 and post-M2, were $-23{,}233$ and $-17{,}704$ deg·cm^2/dmol in 40% TFE, and $-20{,}109$ and $-17{,}782$ deg·cm^2/dmol in 1% SDS, respectively. These values correspond to helicity values of 70% and 52% in 40% TFE and 60% and 52% in 1% SDS (Wu et al., 1981). Because the CD signal of pre-M0 was very low in both 40% TFE/water and in 1% SDS, it could not be attributed to any particular structure. In membrane peptides, the contributions of N- and C-termini blocking to α-helicity has been

Table 1. *Sequences and designations of the peptides investigated*

No.	Designation	Modification	Sequence
1	Pre-M0	**X** = H	**X**-HN-^{36}**S R Q R A R L V S K E G R C N I E F G N V D**^{57}-COOH
2	NBD-pre-M0	**X** = NBD	
3	M0	**X** = H	**X**-HN-^{58}**A Q S R F I F F V D I W T T V L D L K W R Y K**^{80}-COOH
4	NBD-M0	**X** = NBD	
5	Rho-M0	**X**-Rho	
6	Post-M2	**X** = H, **Y** = COOH	**X**-HN-^{198}**A V I S K R G G K L C L L I R V A N L R K S L L I G**^{223}-CO-**Y**
7	NBD-post-M2	**X** = NBD, **Y** = OH	
8	NBD-C-post-M2	**X**-H, **Y** = NH$(CH_2)_2$-NH-NBD	
9	Rho-post-M2	**X**-Rho, **Y** = OH	

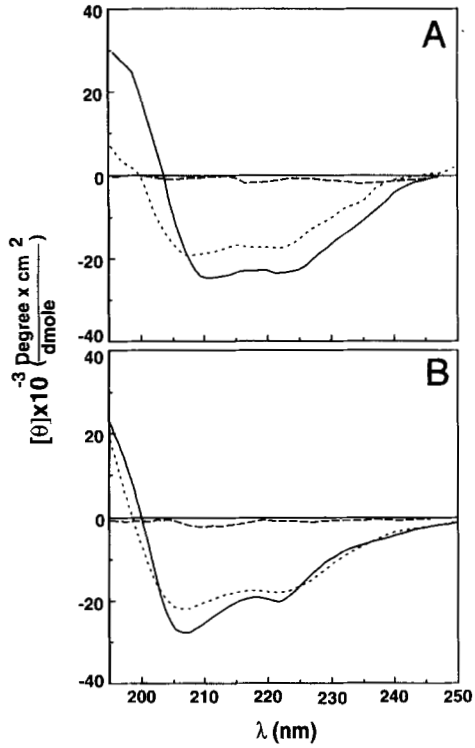

Fig. 1. CD spectra of ROMK1 peptides. Spectra were taken at peptide concentrations of 1.5–2.0 × 10^{-5} M. Symbols: M0 (—); post-M2 (---); pre-M0 (– – –). **A:** CD of peptides in 40% TFE. **B:** CD of peptides in 1% SDS.

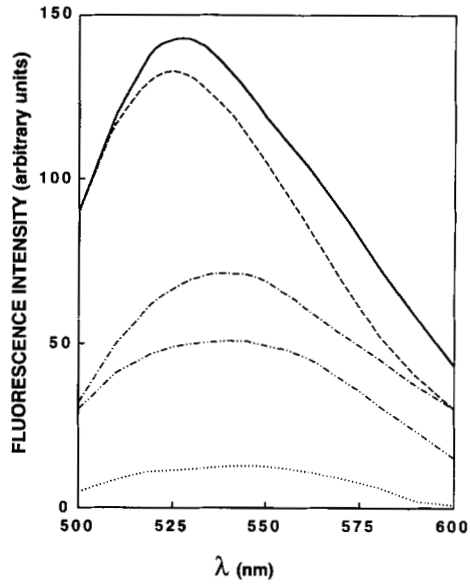

Fig. 2. Fluorescence emission spectra of 0.1 μM NBD-labeled molecules. Spectra were determined in the presence of 460 μM PC vesicles in buffer composed of 50 mM HEPES-SO_4^{2-}, pH 6.8. The excitation wavelength was set at 470 nm. Emission was scanned from 500–600 nm. Symbols: M0 in buffer (· · · ·); M0 with liposomes (—); post-M2 in buffer (– · · – · ·); post-M2 with liposomes (– – –); pre-M0 in buffer and with liposomes (– · – ·).

shown to be small in comparison to that observed in soluble peptides (Shai et al., 1990; Oren & Shai, 1996).

Membrane localization of the segments

Fluorescence measurements of NBD-labeled peptides

Whether M0 and post-M2 are localized in the membrane was examined. The NBD probe was used to facilitate determination of the environment of the peptides' termini in the membrane-bound state, because its fluorescence intensity is sensitive to the dielectric constant of its surroundings. This probe has already been used in polarity and binding experiments (Baidin & Huang, 1990; Rapaport & Shai, 1991; Pouny et al., 1992). Fluorescence emission spectra of the three NBD-labeled ROMK1 peptides were measured in aqueous solutions and in the presence of PC vesicles. In buffer, all three NBD-labeled segments exhibited fluorescence emission maxima around 550 nm (Fig. 2), which agrees with emission wavelength maxima reported previously for NBD derivatives in hydrophilic environments (Rajarathnam et al., 1989; Rapaport & Shai, 1991; Pouny et al., 1992; Gazit & Shai, 1993b). However, in the presence of PC vesicles at pH 6.8, blue shifts were exhibited in the fluorescence emission maxima of NBD-labeled M0, λ_{max} = 525 ± 1 nm, and post-M2, λ_{max} = 527 ± 2 nm, which were concomitant with increases in their fluorescence intensities (Fig. 2). Post-M2 labeled at its C terminus exhibited the same blue shift as the N terminus labeled post-M2 and therefore is not shown in Figure 2. With the addition of vesicles to pre-M0, it did not exhibit a blue shift or an increase in its quantum yield. Thus, it was concluded that pre-M0 does not interact with the membrane. Similar magnitudes of blue shifts are observed when surface-active NBD-labeled peptides interact with phospholipid membranes (Frey & Tamm, 1990; Rapaport & Shai, 1991; Pouny et al., 1992) and are consistent with the NBD probe being located near the surface of the membrane (Rajarathnam et al., 1989). However, we cannot rule out the possibility that the environment of the NBD moiety was also affected by the intermolecular organization of the membrane-bound peptide. In these experiments, the lipid/peptide molar ratio was consistently maintained at an elevated level (3875:1), so that the spectral contribution of free peptide would be negligible.

Tryptophan quenching with brominated phospholipids

A tryptophan residue in the natural sequence of a protein or peptide can serve as an intrinsic probe for the localization of the peptide within the membrane. M0 contains two tryptophans, one in the middle of the peptide and the other close to the C terminus. The greatest quenching of tryptophan fluorescence was observed with 6,7-BrPC and to a lesser degree with 9,10-BrPC (Fig. 3). Quenching of fluorescence was not observed with 11,12-BrPC, which indicated that the peptide was surface localized.

Enzymatic digestion of membrane-bound peptides

The susceptibility of membrane-bound M0 and post-M2 to proteolytic digestion by proteinase K was investigated using PC SUV vesicles. At the lipid/peptide molar ratios tested, almost all the peptides are bound to the vesicles, as revealed from the binding isotherms. Figure 4 shows the maximal fluorescence intensity of the peptides as they are added to the vesicles. This increase signifies binding of the peptides to the vesicles. Addition of proteinase K to the vesicle-bound peptides caused a decrease in the maximal

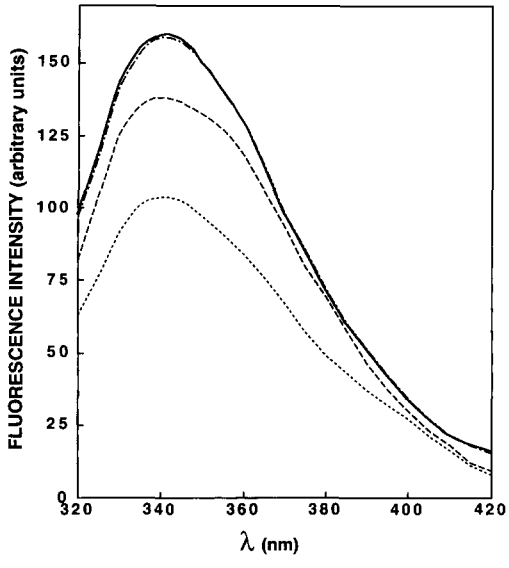

Fig. 3. Fluorescence emission spectra of 0.25 μM M0. Spectra were determined in the presence of 184 μM BrPC or PC vesicles in buffer composed of 50 mM HEPES-SO_4^{2-}, pH 6.8. The excitation wavelength was set at 280 nm. Emission was scanned from 320–420 nm. Symbols: M0 in the presence of: 11,12-BrPC (—); 9,10-BrPC (– – –); 6,7-BrPC (· · ·). For the sake of clarity, M0 with PC vesicles was not included in the figure because it overlaps with 11,12-BrPC.

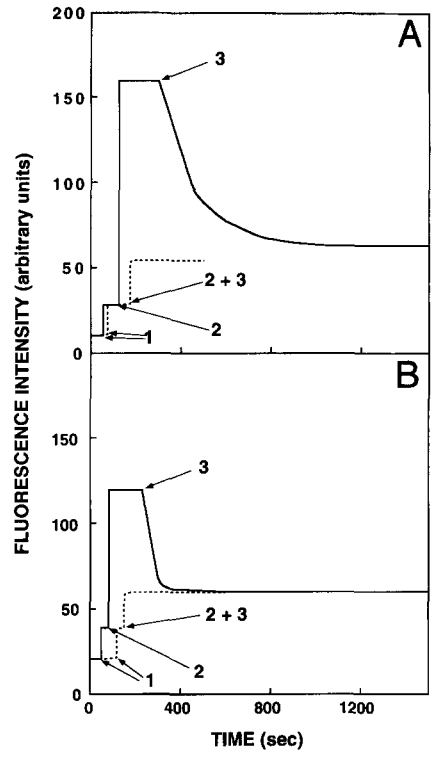

Fig. 4. Digestion of NBD-M0 (**A**) and NBD-post-M2 (**B**) in the presence of vesicles by proteinase K. NBD-labeled peptides (0.1 μM, label 2), PC SUV (184 μM, label 1), and proteinase K (10 μM solution of 0.25 mg/mL, label 3) were mixed in the following order. **A:** Digestion of NBD-M0. ——: first vesicles (1), then peptide (2), and finally enzyme (3). – – – –: first vesicles (1), then peptide (2) premixed with the enzyme (3), and then the two of them together added to the vesicles. **B:** Digestion of NBD-post-M2 as described in Figure 6A.

fluorescence intensity. As seen from the figure, the addition of digested peptides to PC SUV had only a slight effect on the fluorescence intensity. The levels of the fluorescence intensities in the later case were similar to the fluorescence obtained by the addition of proteinase K to the bound peptides. Similar results were obtained with post-M2 labeled at either its N- or C-terminal amino acids. These results indicate that the peptides are not deeply buried within the hydrophobic environment of the vesicles, in contrast, for example, to transmembrane domains derived from δ-endotoxin (Gazit & Shai, 1993a) or the *Shaker* K^+ channel (Peled-Zehavi et al., 1996), which, in the presence of vesicles, were not cleaved by proteinase K.

Binding experiments

The affinity of the segments toward phospholipid membranes was determined by binding experiments (see Materials and methods). The resulting increases in the fluorescence intensities of the NBD-labeled peptides were plotted as a function of the lipid:peptide molar ratios (see Figs. 5A and 6A for NBD-M0 and NBD-post-M2, respectively). Binding isotherms were analyzed as partition equilibria as described in Materials and methods. The curve that results from plotting X_b^* versus free peptide, C_f, is referred to as the conventional binding isotherm. The binding isotherms obtained for NBD-M0 and NBD-post-M2 are presented in Figures 5B and 6B, respectively. The surface partition coefficient of each peptide, K_p^*, was estimated by extrapolating the initial slope of its binding curve to a zero C_f value. The estimated surface partition coefficients, K_p^*, of the NBD-labeled peptides are 1.3×10^5 M^{-1} and 6×10^3 M^{-1} for NBD-M0 and NBD-post-M2, respectively, and the calculated free energies of binding ($\Delta G_{binding}$) (Reynolds et al., 1974) are 9.4 and 7.6 Kcal/mol for NBD-M0 and NBD-post-M2, respectively. The values obtained are high and are typical of surface active peptides (Rizzo et al., 1987; Stankowski & Schwarz, 1990; Rapaport & Shai, 1991; Thiaudiere et al., 1991; Pouny et al., 1992).

The shape of a binding isotherm of a peptide can provide information on the organization of the peptide within the membrane (Schwarz et al., 1987). The binding isotherms of both NBD-M0 and NBD-post-M2 with the vesicles are straight lines, indicating noncooperativity in the binding process.

Fluorescence energy transfer studies

The curvature of a binding isotherm may indicate whether a particular peptide can form large aggregates cooperatively. Whether M0 and post-M2 can self-associate or form heteroaggregates with each other within membranes at low peptide/lipid molar ratios was evaluated by RET measurements as described previously (Pouny et al., 1992). For this purpose, the segments were labeled selectively at their N-terminal amino acid, with either NBD (an energy donor) or Rho (an energy acceptor) (Table 1). In the presence of PC phospholipid vesicles (156 μM), addition of the various acceptors (final concentration of 0.04–0.12 μM) to the various donors (final concentration of 0.04 μM) quenched the donor's emission and increased the acceptor's emission, which is consistent with energy transfer (Fig. 7). The energy transfer was calculated and plotted versus the acceptor/lipid molar ratio (Fig. 8). In these experiments, the lipid/peptide molar ratios were kept high (3,900:1–

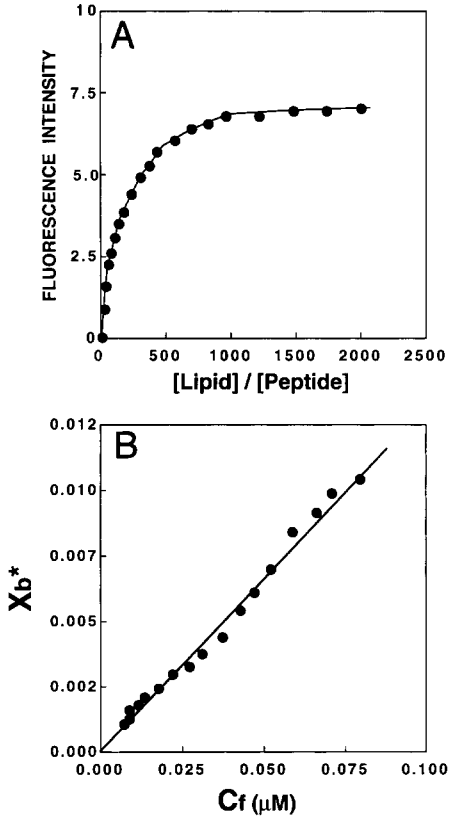

Fig. 5. Increases in the fluorescence of NBD-M0 upon titration with PC vesicles (**A**), and the resulting binding isotherm (**B**). NBD-M0 (0.1 μM) was titrated with PC SUV with the excitation set at 470 nm and the emission recorded at 530 nm. The experiment was performed at room temperature in 50 mM Na_2SO_4, 25 mM HEPES-SO_4^{-2}, pH 6.8. The binding isotherm was derived from A by plotting X_b^* (molar ratio of bound peptide per 60% lipid) versus C_f (equilibrium concentration of free peptide in the solution).

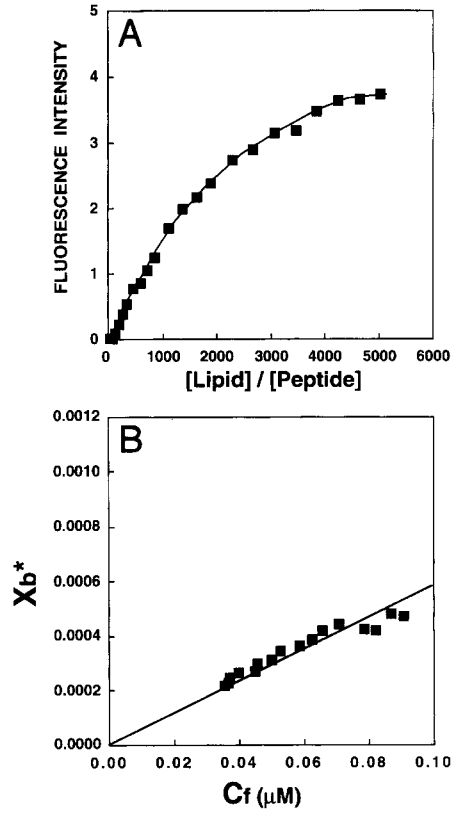

Fig. 6. Increases in the fluorescence of NBD-post-M2 with increasing lipid/peptide molar ratio of PC vesicles (**A**), and the resulting binding isotherm (**B**). See experimental details in Figure 5.

1,300:1) (1) to ensure that most of the peptides would be in their membrane-bound state, and (2) to ensure a low surface density of donors and acceptors, which would reduce energy transfer between unassociated peptide monomers. Because the acceptor peptide was added only after the donor peptide was already bound to the membrane, any association in solution of the peptides was prevented. In order to confirm that the observed energy transfer was due to the peptides' association, the energy transfer efficiencies observed for M0 and post-M2 were compared with those expected for randomly distributed membrane-bound donors and acceptors (Fig. 8). The random distribution was calculated as described by Fung and Stryer (1978) and assumed that 51 Å is the R_0 value for the NBD/Rho donor/acceptor pair (Gazit & Shai, 1993b). Figure 8 illustrates the existence or the lack of energy transfer between the various peptides in their membrane-bound state. The energy transfer observed with the M0/post-M2 donor/acceptor pair was higher than that calculated for a random distribution and was independent of which peptide served as a donor or as an acceptor. Reversal of the donor and the acceptor yielded similar values of RET (Fig. 8). A change in the emission spectrum was not observed when an equal amount of unlabeled acceptor was added instead of the rhodamine-labeled acceptor (data not shown). This suggested that the peptides were associated, rather than randomly distributed, throughout the membrane. With M0/M0 or post-M2/post-M2 pairs, a slight decrease in the emission spectrum of the NBD group (at 530 nm) was obtained independent of whether unlabeled or Rho-labeled M0 or Rho-labeled post-M2 served as acceptors (Fig. 7). In the later case, an increase in the emission spectrum at 580 nm was not observed, which implies that neither M0 nor post-M2 are self-associated in their membrane-bound state.

Discussion

During the last two years, several inwardly rectifying K^+ channels have been cloned, their nucleotide sequences determined, and from them the primary amino acid sequences deduced. However, the topology and organization of ROMK1 and other inwardly rectifying channels is still unknown. Such information is important for elucidating the relationship between the structure and function of these channels. Hydropathy plots facilitate determination of the presence of transmembrane segments in integral membrane proteins. The topologies of many membrane proteins have been predicted on the basis of hydropathy plots (reviewed in Sansom & Kerr, 1995). However, interpretation of hydropathy plots is not unambiguous (Guy & Hucho, 1987), and models based on hydropathy plots alone require further study, e.g., nAChR (Ortells & Lunt, 1994), voltage-gated potassium channels (Catterall, 1988), glutamate receptor (Wo & Oswald, 1995), and cyclic nucleotide gated channels (Henn et al., 1995). In the present study, the structure in hydrophobic environments, affinity to phospholipid membranes, and organization within phospholipid membranes of fragments de-

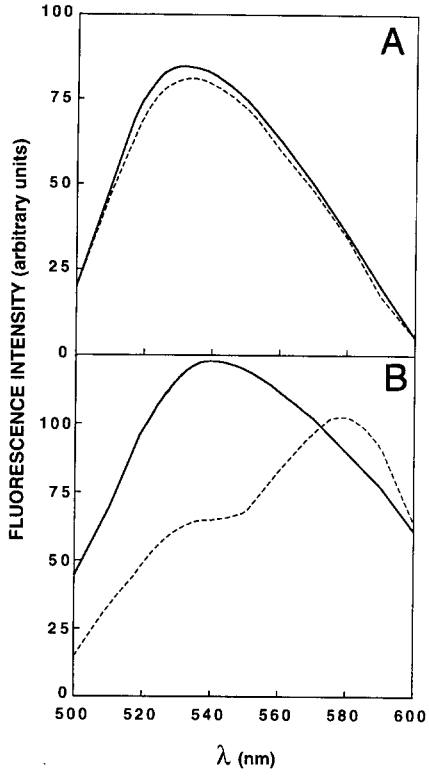

Fig. 7. Fluorescence energy transfer dependence on Rho-peptide (acceptors) concentration using PC LUV. The spectrum of NBD-post-M2 (0.04 μM), the donor peptide, was determined in the absence (—) and presence (– – –) of 0.04 μM of Rho-labeled acceptor peptide. Each spectrum was recorded in the presence of PC vesicles (156 μM) in 50 mM Na_2SO_4, 25 mM HEPES-SO_4^{2-}, at pH 6.8. The excitation wavelength was set at 460 nm. **A:** In the presence of Rho-post-M2. **B:** In the presence of Rho-M0. The spectra of Rho-labeled peptides in the presence of vesicles and unlabeled M0 were subtracted from all the corresponding spectra.

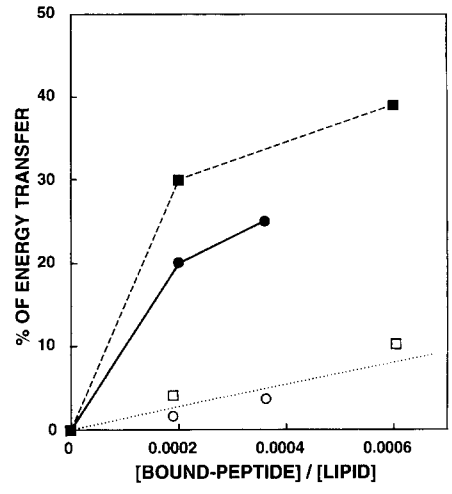

Fig. 8. Theoretically and experimentally derived percentage of energy transfer. The percentage of energy transfer was calculated as described in Materials and methods, and was plotted versus the molar ratio between the bound-acceptor and the lipids. The amounts of lipid-bound acceptor (Rho-peptides), C_b, at various acceptor concentrations were calculated from the binding isotherms as described previously (Pouny et al., 1992). Symbols: ■, NBD-post-M2/Rho-M0; ●, NBD-M0/Rho-post-M2; □, NBD-post-M2/Rho-post-M2; ○, NBD-M0/Rho-M0; – – – –, random distribution of the monomers (Fung & Stryer, 1978), assuming an R_0 of 51 Å.

rived from the N and C termini of ROMK1 K^+ channel were studied. It has been demonstrated that the polypeptide fragments of several membrane proteins behave as independent folding domains and that such fragments of proteins can be functionally recombined in vitro and in vivo (Huang et al., 1986; Popot et al., 1987; Stühmer et al., 1989; Bibi & Kaback, 1990; Kahn & Engelman, 1992; Maggio et al., 1993; Zen et al., 1994; Ridge et al., 1995).

Localization of M0 and post-M2 in their membrane-bound state was evaluated by three methods. Based on NBD shift (Fig. 2), tryptophan quenching with brominated phospholipids (Fig. 3), and enzymatic cleavage (Fig. 4), it was demonstrated that both M0 and post-M2 have high affinity for phospholipid membranes and at membrane surfaces, rather than comprising part of the soluble domains of the channel or being localized in a transmembrane orientation. M0 was studied by a shift in the maximum emission wavelength of an NBD probe located at its N terminus and two tryptophan residues, one in the middle of the peptide and the other near the C terminus. All three markers showed surface localization. M0 contains two tryptophan residues in two different locations. Because the greatest quenching was achieved with 6,7-BrPC and no quenching was achieved with 11,12-BrPC of phospholipid-associated M0, both tryptophans on average are surface localized. Such general assumptions have been made for other proteins that contain more than one tryptophan (Gonzalez-Manas et al., 1992; Rodionova et al., 1995). A shift in the maximum wavelength of an NBD probe located at either the N or C terminus of phospholipid-associated post-M2 also indicated a surface localization of the peptide. Enzymatic cleavage experiments were in agreement with this conclusion, because the topology of many membrane proteins has been demonstrated by proteinase K treatment (Gerbl-Rieger et al., 1992; Kerppola & Ames, 1992; Muller et al., 1993; Lin & Addison, 1994). These results are in agreement with the hydropathy plots that indicated intermediate hydrophobicity of the corresponding regions in ROMK1 and, therefore, predict that these regions will not be membrane spanning (Taglialatela et al., 1994).

Determination of the secondary structure of M0 and post-M2 revealed that both consist of predominantly α-helices when in a membrane mimetic environment (40% TFE, 1% SDS; Fig. 1). Under similar conditions, the structure of pre-M0 could not be interpreted because the peptide did not yield any significant CD signal. The structural and topologic data reported herein for M0 and post-M2 may facilitate in the modeling of the structure of the core region of the ROMK1 channel. In support of this, recent studies have shown a correlation between the structure and organization of synthetic peptides and those of their parent molecules. Such studies were performed with both soluble (Jaenicke, 1991; Kippen et al., 1994) and membrane proteins (Kaback, 1992; Kahn & Engelman, 1992; Lemmon et al., 1992; Lomize et al., 1992; Pervushin & Arseniev, 1992; Adair & Engelman, 1994). Other recent studies showed that various synthetic segments from bacteriorhodopsin (Barsukov et al., 1992), the pore region of δ-endotoxin (Gazit & Shai, 1993a), and *Bacillus thuringiensis* var. *israelensis* cytolytic toxin (CytA) (Gazit & Shai, 1993b; Li et al., 1996) also adopt conformations similar to those of their corresponding segments within the intact proteins, as determined by X-ray data.

We further demonstrated that M0 and post-M2 are capable of coassembling when bound to phospholipid membranes. RET studies revealed that membrane-bound M0 and post-M2 do not self-

associate, but rather coassemble (Figs. 7, 8). For example, a high energy transfer (~30%) was already detected with NBD-post-M2/Rho-M0 pairs at a peptide/lipid molar ratio of 1:5,000 [after correction for bound acceptor using binding isotherms, as has been described previously (Pouny et al., 1992)]. If a random distribution of these peptides had occurred, an energy transfer of ~3% would have been expected (Fig. 8). Furthermore, based on previous calculations (Tank et al., 1982; Vaz et al., 1981), the following calculations were made. The diffusion coefficients of phospholipids in fluid bilayers are approximately 1.1×10^{-8}–3×10^{-8} cm^2/s (Tank et al., 1982; Vaz et al., 1981). For the excited state lifetime of the donor NBD, $\tau = 7.4 \times 10^{-9}$ s (Chattopadhyay & Mukhrjee, 1993), the mean distance diffused during the lifetime of the donor, r, derived from the equation:

$$r = [4D\tau_0]^{1/2},$$

is approximately 1.8–3 Å, which is small compared with the mean distance between the donor and acceptor in our case (253–440 Å). Thus, the monitored RET appears to be due to association, and not to random distribution. Because both M0 and especially post-M2 are positively charged, it might be argued that they cannot self-associate due to their net positive charge. However, positively charged membrane-seeking peptides, such as dermaseptin B, can self-assemble in membranes (Strahilevitz et al., 1994). Therefore, the lack of self-aggregation in M0 and post-M2 could not be due solely to charge repulsion. Such recognition, leading to coassembly between membranous sequences, has been demonstrated in other membrane proteins, such as glycophorin A (Lemmon et al., 1992), bacteriorhodopsin (Kahn & Engelman, 1992), the lactose permease of *Escherichia coli* (Sahin-Toth et al., 1992), helix I and helix II of *B. thuringiensis* var. *israelensis* (Gazit & Shai, 1993b), and ion channels (Peled & Shai, 1993; Babila et al., 1994; Ben-Efraim et al., 1994; Papazian et al., 1995; Planells-Cases et al., 1995; Pouny & Shai, 1995; Peled-Zehavi et al., 1996). These and other examples (reviewed in Lemmon & Engelman, 1992; Shai, 1995) suggest that transmembrane segments in other proteins also can contribute to the specific recognition and assembly.

In summary, it was demonstrated that, in a membrane-bound state, synthetic peptides corresponding to the N and C termini of the inwardly rectifying ROMK1, are membrane-bound, surface-localized, and preferentially coassembled segments, rather than randomly distributed. Therefore, we propose that certain domains from the N and C termini are capable of interacting with membranes and with each other, and that this interaction might contribute to the organization and stabilization of the protein in the membrane that culminates in the formation of a functional K^+ channel (Fig. 9B). These findings are also in agreement with experimental evidence in which exchange of the C terminus altered pore properties, which suggested that, in inwardly rectifying channels, parts of the C terminus are likely to be in the membrane and that the C terminus seems to make a major contribution to the pore (Taglialatela et al., 1994; Pessia et al., 1995).

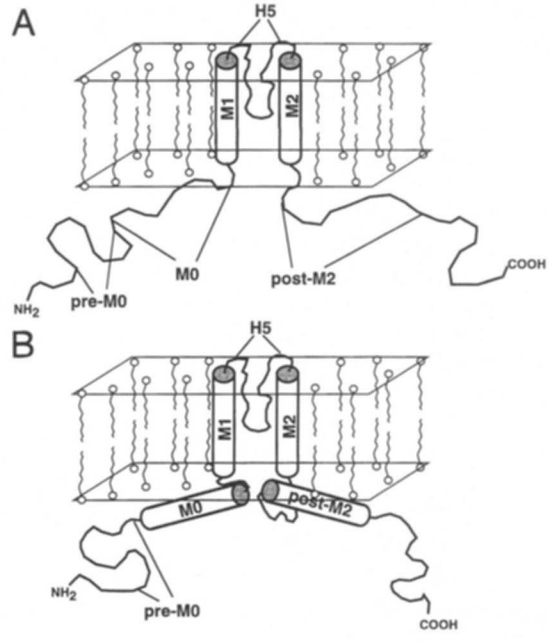

Fig. 9. Schematic representation illustrating the proposed topology of the ROMK1 channel as predicted by Kyte and Doolittle (1982) hydropathy plot (**A**) and based on the results obtained in the present study (**B**).

Materials and methods

Materials

[1]BOC-(amino-acid)-Pam resins were purchased from Applied Biosystems (Foster City, California) and BOC amino acids were obtained from Peninsula Laboratories (Belmont, California). Other reagents for peptide synthesis were obtained from Sigma. PC was purchased from Lipid Products (South Nutfield, UK). Cholesterol (extra pure), purchased from Merck (Darmstadt, Germany), was recrystallized twice from ethanol. BrPCs were purchased from Avanti Polar-Lipids, Inc. Rho-Su was obtained from Molecular Probes (Eugene, Oregon). NBD-F was obtained from Sigma. All other reagents were of analytical grade. Buffers were prepared using double glass-distilled water.

Methods

Peptide synthesis, fluorescent-labeling, and purification

Peptide synthesis was done using a solid phase method on Pam-amino acid resin (0.15 meq) (Merrifield et al., 1982), as described previously (Shai et al., 1990). Double coupling was conducted with freshly prepared HOBT active esters of BOC amino acids. The synthetic polypeptides were purified to a chromatographic homogeneity of >98% by RP-HPLC on an analytical C_{18} Vydac column 4.6 mm × 250 mm (300-Å pore size). The column was eluted in 40 min using linear gradients of acetonitrile in water in the presence of 0.1% trifluoroacetic acid (TFA) (v/v). The flow rate was 0.6 mL/min and the gradients were: 10–80% for post-M2 and M0, and 5–60% for pre-M0. The peptides were subjected to amino acid analysis to confirm their composition.

The N terminus of the resin-bound polypeptide was labeled in its fully protected form as follows: resin-bound peptide (30–40 mg, i.e., 10–25 μmol) was treated with TFA (50% v/v in methylene chloride) to remove the BOC-protecting group from the N-terminal amino group of the attached peptide (Rapaport & Shai, 1991). The resin-bound peptides were then reacted with either (1) 5–7 equivalents of Rho-Su in DMF containing 3% v/v triethylamine or (2) 5–7 equivalents of NBD-F in DMF. These reactions led to the formation of resin-bound N^1-Rho or N^1-NBD peptides, respec-

tively. After 24 h, the resins were washed thoroughly with DMF and then with methylene chloride. After the formyl-protecting group was removed from the tryptophan residues, the peptides were cleaved from the resin with HF. The cleaved peptides were precipitated with ether and purified by RP-HPLC as described above. Labeling of post-M2 at its C terminus was performed as described previously (Rapaport & Shai, 1991). Briefly, resin-bound post-M2 (15 mg resin) was treated with 150 μL of ethylene diamine in DMF (1:1 (v/v)) for 48 h, resulting in transamidation of the C-terminal carboxylate group of the glycine residue located at the C terminus of the peptide. By this procedure, a post-M2 analogue was obtained in which all the protecting groups remained attached, but whose C-terminal residue was modified by an amino groups. This protected peptide was extracted from the resin by washing with DMF, and then precipitated with dry ether. The protected peptide was then reacted with NBD-F (2 equivalents) in DMF for 5 h, and finally subjected to HF cleavage and purified by RP-HPLC as described above. Peptide concentrations were determined by amino acid analysis and fluorescence emission.

Preparation of SUV

SUV were prepared from PC by sonication. SUV were used in the NBD shift experiments, tryptophan quenching, binding experiments, and CD spectroscopy to decrease light scattering effects. Briefly, dry lipid and cholesterol were dissolved in $CHCl_3$:MeOH (2:1 v/v) to yield mixtures that contained 10% w/w of cholesterol. Cholesterol was included to reduce the curvature of the SUV (Lelkes, 1984). The solvents were evaporated under a stream of nitrogen and the lipids (at a concentration of 7.2 mg/mL) were resuspended in buffer (50 mM Na_2SO_4, 25 mM HEPES-SO_4^{-2}, pH 6.8) by vortex mixing. The resulting lipid dispersion was sonicated (10–30 min) in a bath-type sonicator (G1125SP1 Sonicator, Laboratory Supplies Company Inc., New York) until the turbidity had cleared. The lipid concentration of the solution was determined by phosphorus analysis (Bartlett, 1959). Vesicles were visualized after negative staining with uranyl acetate, using a JEOL JEM 100B electron microscope (Japan Electron Optics Laboratory Co., Tokyo, Japan). Vesicles were shown to be unilamellar, with an average diameter of 20–40 nm (Papahadjopoulos & Miller, 1967; Rapaport & Shai, 1992). Brominated liposomes, prepared by mixing together PC and BrPC and cholesterol, were dissolved in $CHCl_3$:MeOH (2:1, v/v) to yield mixtures that contained 65% PC, 25% BrPC, and 10% cholesterol (w/w).

Preparation of LUV

LUV were used in the resonance energy transfer experiments in order to increase the distance between donor and acceptor molecules on two opposite sites of a vesicle, and were prepared from phospholipids by extrusion (Hope et al., 1985). Dry lipids were hydrated in buffer and dispersed by vortexing to produce multilamellar vesicles. The lipid suspension was frozen-thawed ten times and then extruded through polycarbonate membranes three times, with 0.4-μm pores, and then eight times with 0.1-μm pores (Poretics Corp., Livermore, California). The size distribution of the vesicles was determined by dynamic light scattering in a Malvern 4700 submicron particle analyzer. The mean diameter was found to be 113 nm. The lipid concentrations of the liposome suspensions were determined by phosphorus analysis (Bartlett, 1959).

CD spectroscopy

The CD spectra of the peptides were measured in 40% TFE and 1% SDS in PBS buffer using a Jasco J-500A spectropolarimeter that had been calibrated with (+)-10-camphorsulfonic acid. The spectra were scanned at 23 °C in a capped, quartz optical cell with a 0.5-mm path length. Spectra were obtained at wavelengths from 250 to 200–190 nm. Four scans were performed at a scan rate of 20 nm/min, with a sampling interval of 0.2 nm and a peptide concentration of 15–20 μM.

Fractional helicities (Greenfield & Fasman, 1969; Wu et al., 1981) were calculated as follows:

$$f_h = \frac{([\Theta]_{222} - [\Theta]^0_{222})}{[\Theta]^{100}_{222}},$$

where Θ_{222} is the experimentally observed mean residue ellipticity at 222 nm, and values for $[\Theta]^0_{222}$ and $[\Theta]^{100}_{222}$, corresponding to 0% and 100% helix content at 222 nm, were estimated to be 2,000 and 30,000 deg·cm^2/dmol, respectively (Chen et al., 1974; Wu et al., 1981).

NBD fluorescence measurements

NBD-labeled peptides (0.04 nmol) were added to 0.4 mL of buffer (50 mM Na_2SO_4, 25 mM HEPES-SO_4^{-2}, pH 6.8) containing 20 μL (155 nmol) of PC-SUV, thus establishing a lipid/peptide ratio of 3,875:1. Because the fluorescence of the NBD moiety reached its maximum intensity at this lipid/peptide molar ratio, it is assumed that all the peptide was bound to the vesicles. After a 2-min incubation, an emission spectrum of the NBD group was recorded using a Perkin-Elmer LS-50B spectrofluorometer, with the excitation set at 470 nm (5-nm slit), in three separate experiments.

Tryptophan quenching experiments

The environmentally sensitive tryptophan has been used previously in combination with brominated phospholipids for the evaluation of peptide localization in the membrane (Bolen & Holloway, 1990; De Kroon et al., 1990; Gonzalez-Manas et al., 1992). BrPC employed as quenchers of tryptophan fluorescence are suitable for probing the membrane insertion of peptides because they act over a very short distance and do not drastically perturb the membrane. M0 (0.5 nmol), which contains two tryptophan residues, was added to 2 mL of buffer (50 mM Na_2SO_4, 25 mM HEPES-SO_4^{-2}, pH 6.8) containing 40 μL (310 nmol) of PC-SUV, thus establishing a lipid/peptide ratio of 620:1. After a 2-min incubation, an emission spectrum of the tryptophan was recorded using a Perkin-Elmer LS-50B Spectrofluorometer, with the excitation set at 280 nm (5-nm slit), in three separate experiments. Measurements were performed in a 1-cm path-length quartz cuvette in a final reaction volume of 2 mL.

Enzymatic digestion of membrane-bound peptides

NBD-M0 or NBD-post-M2 (0.1μM each) were added to PC SUV (387 μM) in buffer (50 mM Na_2SO_4, 25 mM HEPES-SO_4^{2-}, pH 6.8), followed by the addition of a 10-μL of proteinase K solution (0.25 mg/mL). Fluorescence intensities as a function of time were obtained before and after the addition of the enzyme. In these experiments, the peptide/lipid molar ratio was kept high (3,870:1) to ensure that most of the peptide is bound to the membrane. In control experiments, NBD-M0 and NBD-post-M2 (0.1 μM) were mixed with the enzyme prior to the addition of the

PC SUV to the solution. Fluorescence spectra were obtained at room temperature in a Perkin Elmer LS-50B spectrofluorometer, with the excitation set at 470 nm, using 5-nm slit, and with the emission set at 530 nm, using a 10-nm slit. Measurements were performed in a 0.4-cm path-length glass cuvette in a final reaction volume of 0.4 mL.

Binding experiments

Binding experiments were performed by using the environmentally sensitive NBD fluorophore as a probe for binding to the membrane, as was done previously (Frey & Tamm, 1990; Rapaport & Shai, 1991). Briefly, PC SUV were added successively to 0.1 μM of NBD-labeled M0 or post-M2 at 24 °C. Fluorescence intensities were measured as a function of the lipid/peptide molar ratio on a Perkin-Elmer LS-50B spectrofluorometer, with the excitation set at 470 nm, using a 5-nm slit, and the emission set at 530 nm, using a 10-nm slit, in five separate experiments. To determine the extent of the lipids' contribution to any given signal, the readings taken when unlabeled peptides were titrated with lipid vesicles were subtracted as background from the recorded fluorescence intensities. The binding isotherms were analyzed as partition equilibria (Schwarz et al., 1986; Rizzo et al., 1987; Beschiaschvili & Seelig, 1990; Rapaport & Shai, 1991), using the following formula:

$$X_b^* = K_p^* C_f$$

where X_b^* is defined as the molar ratio of bound peptide per 60% of the total lipid, assuming that the peptides were initially partitioned only over the outer leaflet of the SUV, as suggested previously (Beschiaschvili & Seelig, 1990); K_p^* corresponds to the partition coefficient; and C_f represents the equilibrium concentration of free peptide in the solution. To calculate X_b, F_∞ (the fluorescence signal obtained when all the peptide is bound to lipid) was extrapolated from a double reciprocal plot of F (total peptide fluorescence) versus C_L (total concentration of lipids) (Schwarz et al., 1986). From the fluorescence intensities of unbound peptide, F_0, and bound peptide, F, the fraction of membrane-bound peptide, f_b, could be calculated using the formula:

$$f_b = (F - F_0)/(F_\infty - F_0).$$

From the calculated value of f_b, it is then possible to calculate C_f, as well as the extent of peptide binding, X_b^*. The curves that result from plotting X_b^* versus free peptides, C_f, are referred to as the conventional binding isotherms.

Resonance energy transfer experiments

Peptides were incorporated into PC vesicles as follows. To solutions of PC LUV (10:1 lipid/cholesterol weight ratio and 63 nmoles of phospholipids in 40 μL of buffer) in separate Eppendorf tubes were added DMSO solutions containing 0.016 nmol of each of the NBD-labeled peptides, M0 and post-M2 (donor), (1) alone or (2) followed by the addition of 0.016 and 0.048 nmol of rhodamine-labeled M0 and post-M2 (acceptor). The experiments were repeated three to five times at each concentration, with the standard deviation being ~3%. Prior to the addition of the acceptor molecules, the vesicle solutions containing donor molecules were vortexed thoroughly. After addition of acceptor molecules, the mixtures were diluted to 0.4 mL with 50 mM Na_2SO_4, 25 mM HEPES-SO_4^{-2}, pH 6.8. Fluorescence spectra were obtained at room temperature with either a SLM-8000 spectrofluorometer or a Perkin-Elmer LS-50B spectrofluorometer, with the excitation monochromator set at 460 nm and a 5-nm slit width. Measurements were performed in a 0.4-cm path-length quartz cuvette in a final reaction volume of 0.4 mL. Although the excitation maximum for NBD is 470 nm, a lower wavelength was chosen in order to minimize the excitation of tetramethylrhodamine (Harris et al., 1991).

The efficiency of energy transfer (E) was determined by calculating the decrease in the quantum yield of the donor due to the addition of an acceptor. E was obtained experimentally from the ratio of the fluorescence intensities of the donor in the presence (I_{da}) and in the absence (I_d) of the acceptor at the emission wavelength of the donor, after correcting for membrane light scattering and the contribution of the acceptor's emission. The percentage value of E is given by the following equation:

$$E = (1 - I_{da}/I_d) \times 100.$$

The correction for light scattering was made by subtracting the signal obtained when unlabeled peptides were incorporated into vesicles containing the donor molecules. A correction for the contribution of the acceptor's emission was made by subtracting the signal produced by the acceptor-labeled analogue alone.

Acknowledgments

This research was supported in part by grants from the Joseph Cohn Center for Biomembrane Research, the Basic Research Foundation administered by the Israel Academy of Sciences and Humanities, and the MINERVA Foundation, Munich, Germany.

References

Adair BD, Engelman DM. 1994. Glycophorin A helical transmembrane domains dimerize in phospholipid bilayers: A resonance energy transfer study. *Biochemistry 33*:5539–5544.

Ashford ML, Bond CT, Blair TA, Adelman JP. 1994. Cloning and functional expression of a rat heart KATP channel. *Nature 370*:456–459.

Babila T, Moscucci A, Wang H, Weaver FE, Koren G. 1994. Assembly of mammalian voltage-gated potassium channels: Evidence for an important role of the first transmembrane segment. *Neuron 12*:615–626.

Baidin G, Huang JR. 1990. Fluorescence properties of the Ca^{2+},(Mg^{2+})-ATPase protein of sarcoplasmic reticulum labeled with 7-chloro-4-nitrobenzo-2-oxa-1,3-diazole. *FEBS Lett 259*:254–256.

Barsukov IL, Nolde DE, Lomize AL, Arseniev AS. 1992. Three-dimensional structure of proteolytic fragment 163–231 of bacterioopsin determined from nuclear magnetic resonance data in solution. *Eur J Biochem 206*:665–672.

Bartlett GR. 1959. Phosphorous assay in column chromatography. *J Biol Chem 234*:466–468.

Ben-Efraim I, Bach D, Shai Y. 1993. Spectroscopic and functional characterization of the putative transmembrane segment of the minK potassium channel. *Biochemistry 32*:2371–2377.

Ben-Efraim I, Strahilevitz J, Bach D, Shai Y. 1994. Secondary structure and membrane localization of synthetic segments and a truncated form of the IsK (minK) protein. *Biochemistry 33*:6966–6973.

Beschiaschvili G, Seelig J. 1990. Melittin binding to mixed phosphatidylglycerol/phosphatidylcholine membranes. *Biochemistry 29*:52–58.

Bibi E, Kaback HR. 1990. In vivo expression of the lacY gene in two segments leads to functional lac permease. *Proc Natl Acad Sci USA 87*:4325–4329.

Bolen EJ, Holloway PW. 1990. Quenching of tryptophan fluorescence by brominated phospholipid. *Biochemistry 29*:9638–9643.

Bredt DS, Wang TL, Cohen NA, Guggino WB, Snyder SH. 1995. Cloning and expression of two brain specific inwardly rectifying potassium channels. *Proc Natl Acad Sci USA 92*:6753–6757.

Catterall WA. 1988. Structure and function of voltage-sensitive ion channels. *Science 242*:50–61.

Chattopadhyay A, Mukhrjee S. 1993. Fluorophore environments in membrane-bound probes: A red edge excitation shift study. *Biochemistry 32*:3804–3811.

Chen YH, Yang JT, Chau KH. 1974. Determination of the helix and betta form of proteins in aqueous solution by circular dichroism. *Biochemistry 13*:3350–3359.

Dascal N, Lim NF, Schreibmayer W, Wang W, Davidson N, Lester HA. 1993. Expression of an atrial G-protein-activated potassium channel in *Xenopus* oocytes. *Proc Natl Acad Sci USA 90*:6596–6600.

De Kroon AI, Soekarjo MW, De Gier J, De Kruijff B. 1990. The role of charge and hydrophobicity in peptide–lipid interaction: A comparative study based on tryptophan fluorescence measurements combined with the use of aqueous and hydrophobic quenchers. *Biochemistry 29*:8229–8240.

Frey S, Tamm LK. 1990. Membrane insertion and lateral diffusion of fluorescence-labelled cytochrome *c* oxidase subunit IV signal peptide in charged and uncharged phospholipid bilayers. *Biochem J 272*:713–719.

Fung BK, Stryer L. 1978. Surface density determination in membranes by fluorescence energy. *Biochemistry 17*:5241–5248.

Gazit E, Shai Y. 1993a. Structural and functional characterization of the α5 segment of *Bacillus thuringiensis* δ-endotoxin. *Biochemistry 32*:3429–3436.

Gazit E, Shai Y. 1993b. Structural characterization, membrane interaction, and specific assembly within phospholipid membranes of hydrophobic segments from *Bacillus thuringiensis* var. *israelensis* cytolytic toxin. *Biochemistry 32*:12363–12371.

Gazit E, Shai Y. 1995. The assembly and organization of the α-5 and α-7 helices from the pore-forming domain of *Bacillus thuringiensis* δ-endotoxin. Relevance to a functional model. *J Biol Chem 270*:2571–2578.

Gerbl-Rieger S, Engelhardt H, Peters J, Kehl M, Lottspeich F, Baumeister W. 1992. Topology of the anion-selective porin Omp32 from *Comamonas acidovorans*. *J Struct Biol 108*:14–24.

Gonzalez-Manas J, Lakey JH, Pattus F. 1992. Brominated phospholipids as a tool for monitoring the membrane insertion of colicin A. *Biochemistry 31*:7294–7300.

Greenfield N, Fasman GD. 1969. Computed circular dichroism spectra for the evaluation of protein conformation. *Biochemistry 8*:4108–4116.

Guy RH, Hucho F. 1987. The ion channel of the nicotinic acetyl choline receptor. *Trends Neurosci 10*:318–321.

Harris RW, Sims PJ, Tweten RK. 1991. Kinetic aspects of the aggregation of clostridium perfringens theta-toxin in erythrocyte membrane. A fluorescence energy transfer study. *J Biol Chem 266*:6936–6941.

Henn DS, Baumann A, Kaupp B. 1995. Probing the transmembrane topology of cyclic nucleotide-gated ion channels with a gene fusion approach. *Proc Natl Acad Sci USA 92*:7425–7429.

Hille B. 1992. *Ionic channels of excitable membranes, 2nd ed.* Sunderland, MA: Sinauer Assn, Inc.

Ho K, Nichols CG, Lederer WJ, Lytton J, Vassilev PM, Kanazirska MV, Hebert SC. 1993. Cloning and expression of an inwardly rectifying ATP-regulated potassium channel. *Nature 362*:31–38.

Hope MJ, Bally MB, Webb G, Cullis PR. 1985. Production of large unilamellar vesicles by a rapid extrusion procedure. Characterization of size distribution, trapped volume and ability to maintain a membrane potential. *Biochim Biophys Acta 812*:55–65.

Huang KS, Bayley H, Liao MJ, London E, Khorana HJ. 1986. Refolding of an integral membrane protein: Denaturation, renaturation, and reconstitution of intact bacteriorhodopsin and two proteolytic fragments. *J Biol Chem 256*:3802–3809.

Jaenicke R. 1991. Protein folding: Local structures, domains, subunits, and assemblies. *Biochemistry 30*:3147–3161.

Kaback HR. 1992. The lactose permease of *Escherichia coli*: A paradigm for membrane transport proteins. *Biochim Biophys Acta 1101*:210–213.

Kahn TW, Engelman DM. 1992. Bacteriorhodopsin can be refolded from two independently stable transmembrane helices and the complementary five-helix fragment. *Biochemistry 31*:6144–6151.

Kerppola RE, Ames GFL. 1992. Topology of the hydrophobic membrane-bound components of the histidine permease. *J Biol Chem 267*:2329–2336.

Kippen AD, Arcus VL, Fersht AR. 1994. Structural studies on peptides corresponding to mutants of the major α-helix of barnase. *Biochemistry 33*:10013–10021.

Koyama H, Morishige K, Takahashi N, Zanelli JS, Fass DN, Kurachi Y. 1994. Molecular cloning, functional expression and localization of a novel inward rectifier potassium channel in the rat brain. *FEBS Lett 341*:303–307.

Kubo Y, Baldwin TJ, Jan YN, Jan LY. 1993a. Primary structure and functional expression of a mouse inward rectifier potassium channel. *Nature 362*:127–133.

Kubo Y, Reuveny E, Slesinger PA, Jan YN, Jan LY. 1993b. Primary structure and functional expression of a rat G-protein-coupled muscarinic potassium channel. [See comments]. *Nature 364*:802–806.

Kyte J, Doolittle RF. 1982. A simple method for displaying the hydrophobic character of a protein. *J Mol Biol 157*:105–132.

Lelkes PI. 1984. *Liposome technology*. Boca Raton, Florida: CRC Press.

Lemmon MA, Engelman DM. 1992. Helix–helix interactions inside lipid bilayers. *Curr Opin Struct Biol 2*:511–518.

Lemmon MA, Flanagan JM, Hunt JF, Adair BD, Bormann BJ, Dempsey CE, Engelman DM. 1992. Glycophorin A dimerization is driven by specific interactions between transmembrane α-helices. *J Biol Chem 267*:7683–7689.

Li JD, Koni PA, Ellar DJ. 1996. Structure of the mosquitocidal δ-endotoxin CytB from *Bacillus thuringiensis* ssp. *kyushuensis* and implications for membrane pore formation. *J Mol Biol 252*:129–152.

Lin J, Addison R. 1994. Topology of the *Neurospora* plasma membrane $H^{(+)}$-ATPase. Localization of a transmembrane segment. *J Biol Chem 269*:3887–3890.

Lomize AL, Pervushin KV, Arseniev AS. 1992. Spatial structure of (34–65) bacterioopsin polypeptide in SDS micelles determined from nuclear magnetic resonance data. *J Biomol NMR 2*:361–372.

Maggio R, Vogel Z, Wess J. 1993. Coexpression studies with mutant muscarinic/adrenergic receptors provide evidence for intermolecular "cross-talk" between G-protein-linked receptors. *Proc Natl Acad Sci USA 90*:3103–3107.

Makhina EN, Kelly AJ, Lopatin AN, Mercer RW, Nichols CG. 1994. Cloning and expression of a novel human brain inward rectifier potassium channel. *J Biol Chem 269*:20468–20474.

Merrifield RB, Vizioli LD, Boman HG. 1982. Synthesis of the antibacterial peptide cecropin A (1–33). *Biochemistry 21*:5020–5031.

Muller MM, Vianney A, Lazzaroni JC, Webster RE, Portalier R. 1993. Membrane topology of the *Escherichia coli* TolR protein required for cell envelope integrity. *J Bacteriol 175*:6059–6061.

Oren Z, Shai Y. 1996. A class of highly potent antibacterial peptides derived from pardaxin, a pore-forming peptide isolated from Moses sole fish *Pardachirus marmoratus*. *Eur J Biochem 237*:303–310.

Ortells MO, Lunt GG. 1994. The transmembrane region of the nicotinic acetylcholine receptor: Is it an all-helix bundle? *Receptors Channels 2*:53–59.

Papahadjopoulos D, Miller N. 1967. Phospholipid model membranes structural characteristics of hydrated liquid crystals. *Biochim Biophys Acta 135*:624–638.

Papazian DM, Schwarz TL, Tempel BL, Jan YN, Jan LY. 1987. Cloning of genomic and complementary DNA from *Shaker*, a putative potassium channel gene from *Drosophila*. *Science 237*:749–753.

Papazian DM, Shao XM, Seo SA, Mock AF, Huang Y, Wainstock DH. 1995. Electrostatic interactions of S4 voltage sensor in *Shaker* K^+ channel. *Neuron 14*:1293–1301.

Peled H, Shai Y. 1993. Membrane interaction and self-assembly within phospholipid membranes of synthetic segments corresponding to the H-5 region of the shaker K^+ channel. *Biochemistry 32*:7879–7885.

Peled-Zehavi H, Arkin IT, Engelman DM, Shai Y. 1996. Coassembly of synthetic segments of *Shaker* K^+ channel within phospholipid membranes. *Biochemistry 35*:6828–6838.

Perier F, Radeke CM, Vandenberg CA. 1994. Primary structure and characterization of a small-conductance inwardly rectifying potassium channel from human hippocampus. *Proc Natl Acad Sci USA 91*:6240–6244.

Pervushin KV, Arseniev AS. 1992. Three-dimensional structure of (1–36) bacterioopsin in methanol-chloroform mixture and SDS micelles determined by 2D 1H-NMR spectroscopy. *FEBS Lett 308*:190–196.

Pessia M, Bond CT, Kavanaugh MP, Adelman JP. 1995. Contribution of the C-terminal domain to gating properties of inward rectifier potassium channels. *Neuron 14*:1039–1045.

Planells-Cases R, Ferrer-Montiel AV, Patten CD, Montal M. 1995. Mutation of conserved negatively charged residues in the S2 and S3 transmembrane segments of a mammalian K^+ channel selectively modulates channel gating. *Proc Natl Acad Sci USA 92*:9422–9426.

Popot JL, Gerchman SE, Engelman DM. 1987. Refolding of bacteriorhodopsin in lipid bilayers a thermodynamically controlled two-stage model. *J Mol Biol 198*:655–676.

Pouny Y, Rapaport D, Mor A, Nicolas P, Shai Y. 1992. Interaction of antimicrobial dermaseptin and its fluorescently labeled analogues with phospholipid membranes. *Biochemistry 31*:12416–12423.

Pouny Y, Shai Y. 1995. Synthetic peptides corresponding to the four P regions of *Electrophorus electricus* Na^+ channel: Interaction with and organization in model phospholipid membranes. *Biochemistry 34*:7712–7721.

Rajarathnam K, Hochman J, Schindler M, Ferguson-Miller S. 1989. Synthesis, location, and lateral mobility of fluorescently labeled ubiquinone 10 in mitochondrial and artificial membranes. *Biochemistry 28*:3168–3176.

Rapaport D, Shai Y. 1991. Interaction of fluorescently labeled pardaxin and its analogues with lipid bilayers. *J Biol Chem 266*:23769–23775.

Rapaport D, Shai Y. 1992. Aggregation and organization of pardaxin in phospholipid membranes. A fluorescence energy transfer study. *J Biol Chem 267*:6502–6509.

Reynolds JA, Gilbert DB, Tanford C. 1974. Empirical correlation between hydrophobic free energy and aqueous cavity. *Proc Natl Acad Sci USA 71*:2925–2927.

Ridge KD, Lee SS, Yao LL. 1995. In vivo assembly of rhodopsin from expressed polypeptide fragments. *Proc Natl Acad Sci USA 92*:3204–3208.

Rizzo V, Stankowski S, Schwarz G. 1987. Alamethicin incorporation in lipid bilayers: A thermodynamic study. *Biochemistry 26*:2751–2759.

Rodionova NA, Tatulian SA, Surrey T, Jahnig F, Tamm LK. 1995. Characterization of two membrane bound forms of OmpA. *Biochemistry* 1921–1929.

Sahin-Toth M, Dunten RL, Gonzalez A, Kaback HR. 1992. Functional interactions between putative intramembrane charged residues in the lactose permease of *Escherichia coli*. *Proc Natl Acad Sci USA 89*:10547–10551.

Sansom MSP, Kerr ID. 1995. *Principle of membrane protein structure in biomembranes*. Greenwich, Connecticut: JAI Press Inc., pp 29–78.

Schwarz G, Gerke H, Rizzo V, Stankowski S. 1987. Incorporation kinetics in a membrane, studied with the pore-forming peptide alamethicin. *Biophys J 52*:685–692.

Schwarz G, Stankowski S, Rizzo V. 1986. Thermodynamic analysis of incorporation and aggregation in a membrane: Application to the pore-forming peptide alamethicin. *Biochim Biophys Acta 861*:141–151.

Shai Y. 1995. Molecular recognition between membrane-spanning polypeptides. *Trends Biochem Sci 20*:460–464.

Shai Y, Bach D, Yanovsky A. 1990. Channel formation properties of synthetic pardaxin and analogues. *J Biol Chem 265*:20202–20209.

Shuck ME, Bock JH, Benjamin CW, Tsai TD, Lee KS, Slightom JL, Bienkowski MJ. 1994. Cloning and characterization of multiple forms of the human kidney ROM-K potassium channel. *J Biol Chem 269*:24261–24270.

Stankowski S, Schwarz G. 1990. Electrostatics of a peptide at a membrane/water interface. The pH dependence of melittin association with lipid vesicles. *Biochim Biophys Acta 1025*:164–172.

Strahilevitz J, Mor A, Nicolas P, Shai Y. 1994. Spectrum of antimicrobial activity and assembly of dermaseptin-b and its precursor form in phospholipid membranes. *Biochemistry 33*:10951–10960.

Stühmer W, Conti F, Suzuki H, Wang X, Noda M, Yahadi N, Kubo H, Numa S. 1989. Structural parts involved in activation and inactivation of the sodium channel. *Nature 339*:597–603.

Taglialatela M, Wible BA, Caporaso R, Brown AM. 1994. Specification of pore properties by the carboxyl terminus of inwardly rectifying K^+ channels. *Science 264*:844–847.

Tank DW, Wu ES, Meers PR, Webb WW. 1982. Lateral diffusion of Gramicidine C in phospholipid multibilayers. Effects of cholesterol and high Gramicidin concentration. *Biophys J 40*:129–135.

Thiaudiere E, Siffert O, Talbot JC, Bolard J, Alouf JE, Dufourcq J. 1991. The amphiphilic alpha-helix concept. Consequences on the structure of staphylococcal delta-toxin in solution and bound to lipids. *Eur J Biochem 195*:203–213.

Tytgat J, Vereecke J, Carmeliet E. 1994. Reversal of rectification and alteration of selectivity and pharmacology in a mammalian Kv1.1 potassium channel by deletion of domains S1 to S4. *J Physiol (Lond) 481*:7–13.

Van de Voorde A, Tytgat J. 1995. Transmembrane segments critical for potassium channel function. *Biochem Biophys Res Commun 209*:1094–1101.

Vaz WLC, Kapitza HG, Steumpel J, Sackmann E, Jovin TM. 1981. Translational mobility of glycerophorin in bilayer membranes of dimyristoylphosphatidylcholine. *Biochemistry 20*:1392–1396.

Very AA, Bosseux C, Gaymard F, Sentenac H, Thibaud JB. 1994. Level of expression in *Xenopus* oocytes affects some characteristics of plant inward-rectifying voltage gated K^+ channel. *Pflugers Arch 428*:422–424.

Wo ZG, Oswald RE. 1995. Unraveling the modular design of glutamate-gated ion channels. *TINS 18*:161–168.

Wu CSC, Ikeda K, Yang JT. 1981. Ordered conformation of polypeptides and proteins in acidic dodecyl sulfate solution. *Biochemistry 20*:566–570.

Zen KH, McKenna E, Bibi E, Hardy D, Kaback HR. 1994. Expression of lactose permease in contiguous fragments as a probe for membrane-spanning domains. *Biochemistry 33*:8198–8206.